APPLICATION OF AN ALIGNED AND UNALIGNED SIGNAL PROCESSING TECHNIQUE TO INVESTIGATE TONES AND BROADBAND NOISE IN FAN AND CONTRA-ROTATING OPEN ROTOR ACOUSTIC SPECTRA

Jeffrey Hilton Miles and Lennart S. Hultgren
National Aeronautics and Space Administration
John H. Glenn Research Center at Lewis Field
Cleveland, Ohio 44135, USA

Abstract

The study of noise from a two-shaft contra-rotating open rotor (CROR) is challenging since the shafts are not phase locked in most cases. Consequently, phase averaging of the acoustic data keyed to a single shaft rotation speed is not meaningful. An unaligned spectrum procedure that was developed to estimate a signal coherence threshold and reveal concealed spectral lines in turbofan engine combustion noise is applied to fan and CROR acoustic data in this paper.

Introduction

Interest has been growing in using contra-rotating open rotor (CROR) engines for aircraft propulsion since they are estimated to burn less fuel than equivalent thrust turbofans.[1] CRORs are complex aeroacoustic systems which produce tonal and broadband noise. The determination of tonal and broadband noise components from a total noise signature obtained during testing is an important aspect when studying aircraft noise control parameters and also when validating aircraft noise prediction codes.[2-7] The current status of aircraft turbomachinery aeroacoustics, in general, is discussed in Peake and Parry[8] and the aeroacoustics of CROR systems is discussed in Soulat, Kernemp, Sanjose, and Moreau[7] and Rossikhin, Brailko and Mileshin.[9]

Fan tones from a single set of rotating blade rows on a single shaft can be studied using phase averaging keyed to the shaft rotation speed. This procedure removes the parts of the signal unrelated to the rotation rate. Studying noise from a two-shaft CROR is more challenging since the two shafts are not, in many cases, phase locked. Hence, a need exists to develop effective methods of analyzing CROR noise. A signal processing technique for separating tonal and broadband noise components from CROR data was developed by Sree[10] and was applied by Sree and Stephens[11] to wind-tunnel CROR data obtained at the NASA Glenn Research Center. In addition, this same data set was processed using a two-shaft Vold-Kalman order-tracking filter by Stephens and Vold.[12]

The present paper describes a simple procedure to calculate the tonal components of the noise spectra from CROR tests. The tonal frequencies are identified using the unaligned spectrum procedure discussed by Miles.[13,14] The broadband noise is then obtained by removing the now identified tonal content from the original aligned spectra.

Acoustic Data

The acoustic data used herein are from two rig tests conducted in the NASA Glenn Research Center 9- by 15-ft Low Speed Wind Tunnel.[15] The first set is a baseline test case from the NASA fan trailing edge blowing experiment.[16] This test campaign used a single-shaft modular fan stage in a nacelle with 18 rotor blades and 45 radial stator vanes in order to evaluate exit-guide-vane-noise reduction by filling in fan wakes. The baseline setup used a fan (Fan 1) without blowing capability and thus represented a typical turbofan stage. The acoustic data used herein was measured at a sideline angle of 75.1° for approach conditions (microphone location 30; reading 2338).

The second set of measurements covers some of the ones used by Sree and Stephens[11] and Stephens and Vold.[12] It is from a CROR test that used a baseline, vintage 1990s, blade design, known as F31/A31, whose aerodynamic and acoustic data can be disseminated.[17,18] The test program was conducted by NASA in collaboration with GE Aviation. The F31/A31 blade set consists of 12 front rotor blades and 10 aft rotor blades. Data obtained using this two-shaft blade set is discussed by Sree and Stephens,[11] Stephens and Vold,[12] Elliott,[17] Stephens,[18] Stephens and Envia,[19] and Horvath, Envia, and Podboy.[20] The two shafts are nominally rotating at the same speed,

but they are not phase locked. Sideline acoustic measurements at 90° (microphone location 8, readings 470 and 472, Escort program D074), corresponding to takeoff conditions, were used here.

Uncertainty in the sideline acoustic measurements is estimated to be +/-1 dB.[21]

Data Processing Procedure

Only a brief description of the aligned/unaligned method is given here. More details can be found in papers by Miles.[13,14]

Aligned and Unaligned Spectra

All the spectra and cross-spectra are estimated using Welch's non-parametric method which is based on averaging multiple windowed periodograms using overlapping time sequences.[22] In this procedure the time history is divided into segments. The segment size or length, N, depends on the desired bandwidth resolution, Δf, given by $\Delta f = r_s/N$, where r_s is the sampling rate. To get the aligned spectrum, $G_a(f)$, the time history is duplicated and the cross-spectrum is calculated, i.e. an aligned auto-spectrum (real and positive definite) is actually calculated. To get the deliberately unaligned spectrum, $|G_u(f)|$, the second time history is shifted/displaced at least one segment length and the cross-spectrum is calculated. The unaligned spectrum is the magnitude of this (complex) cross-spectrum and contains only tones and random noise. These tones are present in each of the unmatched segments used to calculate the deliberately unaligned spectrum. All the other spectral values are averaged to smaller and smaller values by the calculation procedure. The spectral estimation parameters are shown in Table 1.

Table 1. Spectral Estimation Parameters

Parameter	Value
Sample rate, r_s, samples/s	200 000
Segment length, N, samples	16 384
Segment length, $T_d = N/r_s$, s	0.08192
Bandwidth resolution, $\Delta f = 1/T_d$, Hz	12.2
Overlap	0.50
Data window type	Hamming
Total sample length, T_{total}, s	15
Displacement shift in samples, $1 \times N$	16 384
Displacement shift, s	0.08192
Number of independent sets, M	363
UMSC threshold (95%), ε^2	0.00824

By varying the time displacement, it was observed that the major unaligned tones largely remained unchanged. However, minor tones showed a slight magnitude variation depending on the displacement. Consequently, the unaligned tonal amplitudes depend weakly on the displacement factor used in the data processing procedure. This is believed to be a consequence of shaft RPM drifts.

The results presented herein were, in general, calculated using a deliberate unalignment time shift with a displacement factor of unity. Consequently, the number of displacement points was 16 384 corresponding to 0.08192 s. Thus one time history was made shorter by removing the first 0.08192 s before calculating the cross spectrum.

Unaligned Magnitude-Squared Coherence

For the case considered herein, where the two signals are simply related by a time shift, the usual magnitude-squared coherence (*MSC*) function reduces to

$$\gamma^2 = |G_u(f)|^2 / G_a(f)^2 , \qquad (1)$$

which, from now on, will be referred to as the unaligned magnitude-squared coherence (*UMSC*). Theoretically the *UMSC*-ranges from zero to unity. A value of zero at a particular frequency would indicate the signal and the displaced signal are uncorrelated while a value of unity would signify that the two signals are perfectly correlated. However, the time series used are finite. Consequently, the *UMSC* will never be zero. Instead, a *UMSC* threshold value, ε^2, is calculated from[13,14]

$$\varepsilon^2 = 1 - (1 - P)^{1/(M-1)} , \qquad (2)$$

where $0 \leq P \leq 1$ is the confidence interval and M is the number of independent sets. If the computed *UMSC* falls below this value at certain frequencies then the two signals are uncorrelated at those frequencies with a confidence level P. $P = 0.95$ is used herein, which corresponds to $\varepsilon^2 = 0.00824$.

Broadband and Tonal Noise Spectra

A common practice to determine the broadband noise spectrum is to set the aligned tones to zero and use a multi-point average to interpolate the missing values. This procedure is not very exact since the decision of which spectrum point is or is not a tone is not well defined. This ad hoc procedure can be improved by selecting the tones to be set to zero based on their

UMSC value. For example, replacing only tones with computed *UMSC* values larger than the 95 percent confidence-level threshold value, obtained from Eq. (2), then using a multi-point averaging technique, leads to a well-defined process that can easily be automated. Here, the four nearest non-tonal spectral values are used. The dominant tonal spectrum can then be obtained by subtracting this broadband spectrum from the original aligned spectrum.

Results

A comparison to existing results[11] for the simpler single-shaft fan-stage configuration is discussed first. This includes a comparison to phase-averaged results (generally considered the gold standard in this case) as well as Sree-method[10] results. Using the insights from these comparisons, two-shaft CROR data is then analyzed and compared to existing results.[11,12]

Single-Shaft Fan Stage

Figure 1(a) shows aligned (black) and unaligned (red and magenta) fan sound pressure level (SPL) spectra, normalized to 1 Hz bin width, for frequencies up to 10 kHz. The red curve shows the threshold-limited unaligned spectrum, where computed values less than $\varepsilon G_a(f)$ have been replaced by this limit value. The magenta curve shows the unaligned spectrum result without applying this lower bound. Figure 1(a) shows that the broadband noise is clearly absent in the deliberately unaligned spectrum. In general, if they are large enough, the tones in the unaligned spectrum appear as tones in the aligned spectrum at the identical frequency. However, the tones in the unaligned spectrum are generally lower than the corresponding tones in the aligned spectrum, occasionally by as much as 3 dB. This loss of tonal energy is believed to be caused by shaft RPM drift since it is more pronounced for higher harmonics. Note that the deliberately unaligned spectrum also identifies tones that are masked by broadband noise. For the subdominant tones, the current method is expected to correctly determine tonal frequencies, while likely underestimating the magnitudes.

Figure 1(b) shows the computed *UMSC* for the 0 to 10 kHz frequency range using a logarithmic scale on the vertical axis. The magenta line indicates the 95 percent confidence level threshold curve ($M = 363$; 50 percent segment overlap). If a point falls below the coherence threshold value, the unaligned signals are independent at that frequency.

Figure 2 compares the current tonal (red) and broadband (blue) spectra with the corresponding results obtained by Sree and Stephens.[11] Panel 2(a) shows the current results obtained by using the *UMSC* threshold criteria for the tones and the multi-point averaging technique for the broadband signature as described above. Panels 2(b) and (c) are replots of the results obtained by Sree and Stephens.[11] Panel 2(b) is their phase-averaged result (Fig. 3, Ref 11) and Panel 2(c) is their Sree-method result (Fig. 4, Ref 11). Good agreement (< 1 dB difference on the strongest tones) with their results (particularly the phase-averaged ones) is shown.

Contra-Rotating Open Rotor

Figure 3(a) shows aligned (black) and unaligned (red and magenta) CROR sound pressure level (SPL) spectra, normalized to 1 Hz bin width, versus frequency for reading 470. Again, the red curve shows the threshold-limited unaligned spectrum, where computed values have been limited from below by $\varepsilon G_a(f)$, and the magenta curve shows the unlimited result. Figure 3(b) shows the corresponding *UMSC* results. Apart from the much richer tonal structure, a striking difference, when comparing the CROR Figure 3(a) with the corresponding singe-shaft fan Figure 1(a), is the much larger tonal-amplitude reduction between the aligned (black) and unaligned (red) spectra for the CROR. This is particularly so for the interaction tones at shaft orders 32, 34, and 42 (these three tones are also the overall strongest tones in the aligned spectra). However, the corresponding reduction for the (fundamental) aft and front rotor blade-passing frequencies (shaft order 10 and 12) are within 1 and 2 dB, respectively. These two observations support the previous inference that the difference in tonal energy between the two spectra is due to RPM drifts, which are larger for the CROR (+/- 20 RPM) than for the single shaft fan (+/- 3 RPM). In addition, even though the RPM drifts for the two CROR shafts somewhat track each other, they are not in sync.

Figure 4 shows CROR tonal (red) and broadband (blue) spectra for reading 470. Panels 4(a) and 4(b) show the current results with a dealignment of one, and one and a half windows, respectively. Due to the loss of tonal energy in the unaligned spectra, it can be seen that certain, but mainly different, tones have been misidentified as broadband in these two examples. However, a good result can be obtained by using information based on more than one displacement case. If the *UMSC* value in at least one case is above the threshold value, then there is a tone

at that particular frequency. The results in Panel 4(c) are obtained by using the computed *UMSC* from both of the displacement cases shown in Panels 4(a) and 4(b). Panel 4(d) is a replot of existing Sree-method results (Fig. 6, Ref 11). The spectra in Panels 4(c) and 4(d) agree quite well.

Figure 5 compares the current tonal (red) and broadband (blue) spectra with the corresponding results obtained by Stephens and Vold.[12] Panel 5(a) shows the current results obtained by using a single displacement of one window length. Panel 5(b) shows the results when applying the *UMSC* threshold criteria using multiple displacement factors (1, 1.5, and 2). Clearly, using multiple displacements improves the tone detection. The most significant frequency range (up to shaft order 80)[11] is well resolved in Panel 5(b). Panels 5(c) and (d) are replots of the results obtained by Stephens and Vold.[12] Panel 5(c) shows their moving-median and modified moving-median (peak-finding) results (Fig. 6a, Ref 12) and Panel 5(d) is their Vold-Kalman-filter results (Fig. 9b, Ref 12). The results shown in Panels 5(b) – (d) are in good agreement.

Concluding remarks

Special signal processing tools are needed to characterize open rotor acoustics. The aligned/unaligned signal processing technique has been applied to fan and counter-rotating open rotor acoustic data. The method offers an effective means of identifying tones in the acoustic data. It will not only detect dominant tones but also tones that may be masked by broadband noise. The use of this method, in combination with magnitude-squared coherence threshold values, leads to a well defined, easily implemented, and effective procedure for extracting, in turn, the broadband and dominant tonal spectra from complex experimental acoustic data sets.

Acknowledgments

Due to the unexpected passing of Dr. Jeffrey Hilton Miles, Dr. Lennart S. Hultgren completed this paper.

References

[1] Guynn, M. D., Berton, J. J., Hendricks, E. S., Tong, M. T., Haller, W. J., and Thurman, D. R., "Initial Assessment of Open Rotor Propulsion Applied to an Advanced Single-Aisle Aircraft," AIAA-2011-7058, September 2011.

[2] Magliozzi, B., Hanson, D. B., and Amiet, R. K., "Propeller and Propfan Noise," *Aeroacoustics of Flight Vehicles: Theory and Practice*, edited by H. H. Hubbard, .Chapter 1, NASA Reference Publication 1258, Vol 1; WRDC Technical Report 90-3052, 1991, pp. 1–64.

[3] Blandeau, V. P. and Joseph, P. F., "Broadband Noise Due to Rotor-Wake/Rotor Interaction in Contra-Rotating Open Rotors," *AIAA Journal*, Vol. **48** (11), November 2010, pp. 2674–2686.

[4] Roger, M., Schram, C., and Moreau, S., "On Open Rotor Blade-Vortex Interaction Noise," AIAA-2012-2216, June 2012.

[5] Sharma, A. and Chen, H., "Prediction of Tonal Aerodynamic Noise from Open Rotors," AIAA-2012-2265, June 2012.

[6] Kingan, M. J., "Open Rotor Broadband Interaction Noise," AIAA-2012-2304, June 2012.

[7] Soulat, L., Kernemp, I., Sanjose, M., and Moreau, S., "Assessment an comparison of tonal noise models for Counter-Rotating Open Rotors," AIAA-2013-2201, May 2013.

[8] Peake, N. and Parry, A. B., "Modern Challenges Facing Turbomachinery Acoustics," *Annual Review of Fluid Mechanics*, Vol. **44** , 2012, pp. 227–248.

[9] Rosikhin, A. A., Brailko, I. A., and Mileshin, V. I., "Numerical investigation of tonal noise of counter-rotating open rotors," *International Journal of Aeroacoustics*, Vol. **13** No. 3&4, 2014, pp. 303–320.

[10] Sree, D., "A novel signal processing technique for separating tonal and broadband noise components from counter-rotating open-rotor acoustic data," *International Journal of Aeroacoustics*, Vol. **12** (1+2), 2013, pp. 169–188.

[11] Sree, D. and Stephens, D. B., "Tone and Broadband Noise Separation from Acoustic Data of a Scale-Model Contra-Rotating Open Rotor," AIAA-2014-2744, June 2014.

[12] Stephens, D. B. and Vold, Håvard, "Order tracking signal processing for open rotor acoustics," Journal of Sound and Vibration, Vol. **333**, 2014, pp. 3818-3830.

[13] Miles, J. H., "Aligned and Unaligned Coherence: A New Diagnostic Tool," Tech. Rep. AIAA-2006-0010, AIAA, 2006, Presented at the 44th AIAA Aerospace Science Meeting, 9-12 Jan 2006 Reno Hilton Reno, Nevada, also NASA/TM–2006-214112.

[14] Miles, J. H., "Estimation of signal coherence threshold and concealed spectral lines applied to detection of turbofan engine combustion noise," *The Journal of the Acoustical Society of America*, Vol. **129** No. 5, May 2011, pp. 3068–3081.

[15] Arrington, E. A. and Gonsalez, J. C., "Flow Quality Improvements in the NASA Lewis Research Center 9- by 15-Foot Low Speed Wind Tunnel," AIAA-1995-2390, July 1995.

[16] Fite, E. B., Woodward, R. P., and Podboy, G. G., "Effect of Trailing Edge Flow Injection on Fan Noise and Aerodynamic Performance," AIAA-2006-2844, 2006.

[17] Elliott, D. M., "Initial Investigation of the Acoustics of a Counter Rotating Open Rotor Model With Historical Baseline Blades in a Low Speed Wind Tunnel," AIAA-2011-2760, June 2011.

[18] Stephens, D. B., "Nearfield Unsteady Pressures at Cruise Mach Numbers for a Model Scale Counter-Rotation Open Rotor," AIAA-2012-2264, June 2012.

[19] Stephens, D. B. and Envia, E., "Acoustic Shielding for a Model Scale Counter-rotation Open Rotor," AIAA-2011-2940; also NASA TM–2012-217227, 2011.

[20] Horvath, C., Envia, E., and Podboy, G. G., "Limitations of Phased Array Beamforming in Open Rotor Noise Source Imaging," AIAA-2013-2098, May 2013.

[21] Envia, E., Tweedt, D. L., Woodward, R. P., Elliot, D. M., Fite, E. B., Hughes, C. E., Podboy, G. G. and Sutliff, D. L., "Fan Noise Prediction," in *Assessment of NASA's Aircraft Noise Prediction Capabiliy,"* editor Dahl, M. D., NASA TP—2012-215653, 2012, pp. 115-156.

[22] Welch, P. D., "The Use of Fast Fourier Transform for the Estimation of Power Spectra: A Method Based on Time Averaging Over Short, Modified Periodograms, "*IEEE Trans-actions on audio and electroacoustics*, Vol. **AU-15** No.2, June 1967, pp. 70–73.

(a)

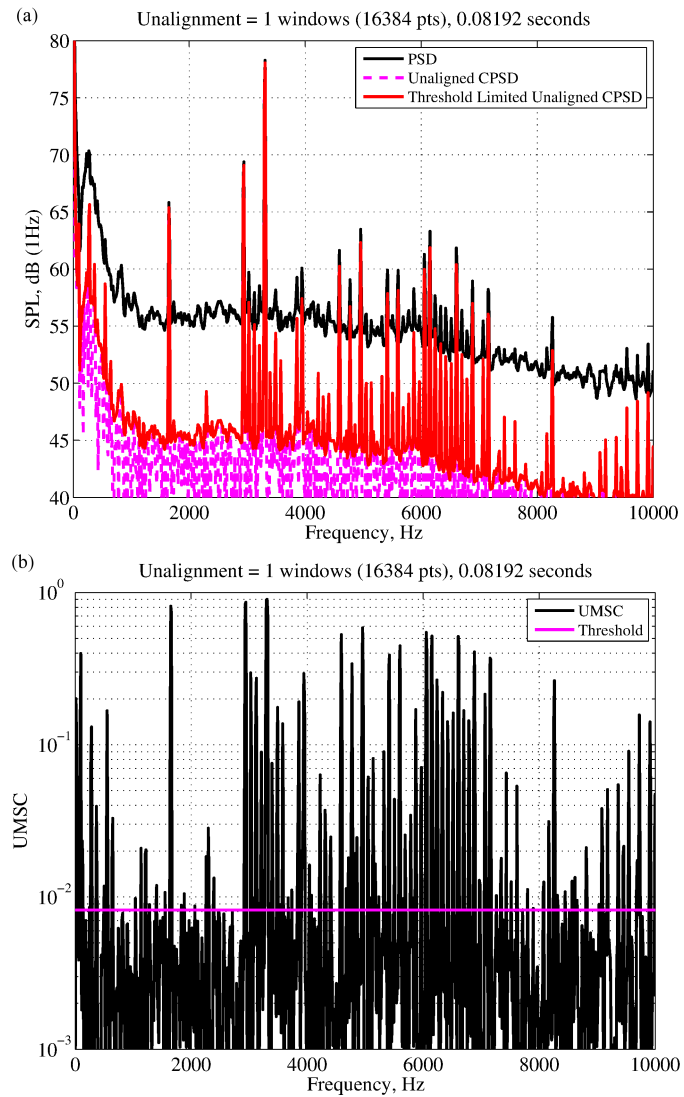Unalignment = 1 windows (16384 pts), 0.08192 seconds

Figure 1. Single-shaft fan results: (a) – aligned (black) and unaligned (red, threshold-limited, and magenta) 1 Hz normalized SPL; (b) – *UMSC* (black) and threshold value (magenta).
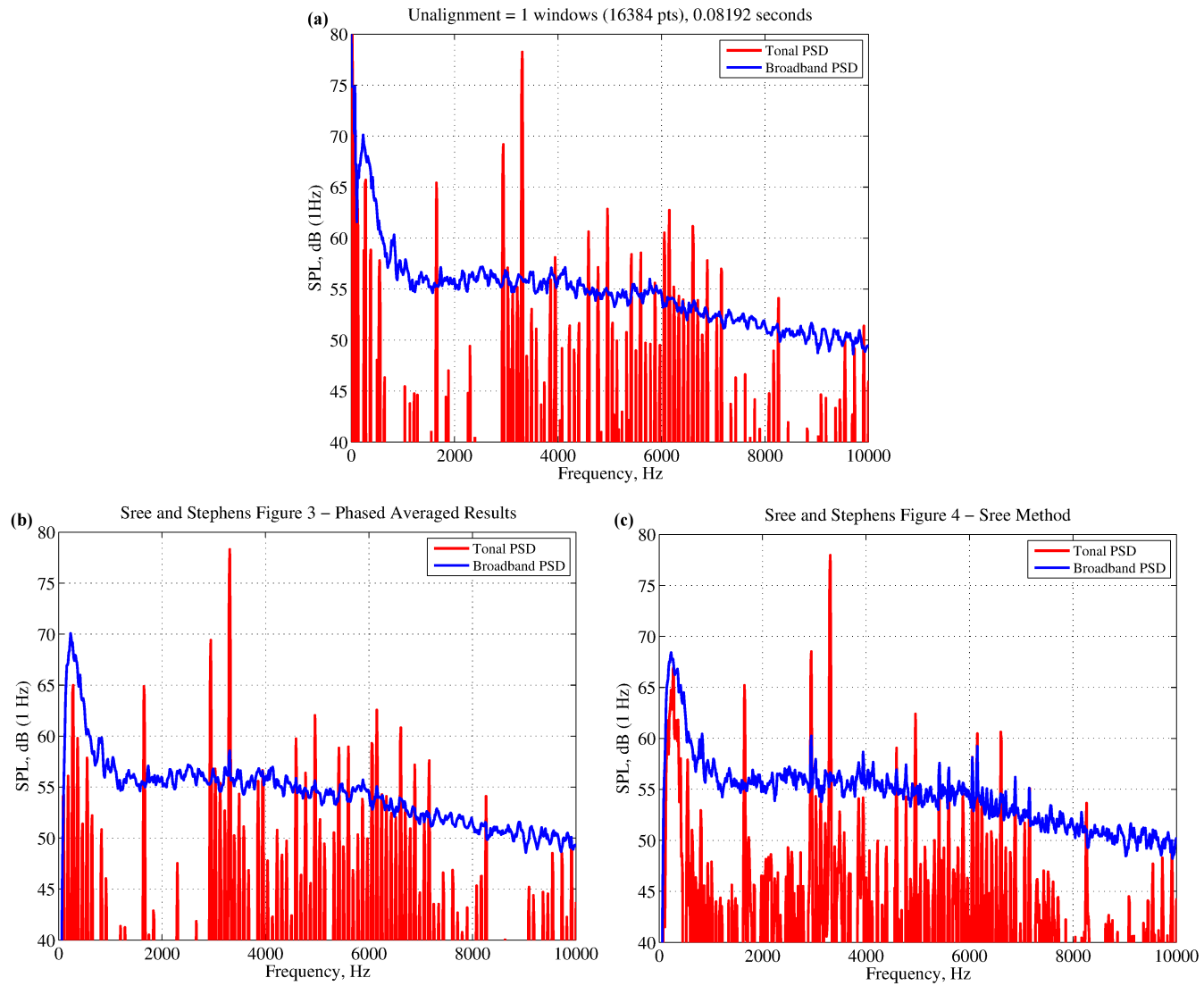
Figure 2. Single-shaft fan tonal (red) and broadband (blue) 1 Hz normalized SPL: (a) – current aligned/unaligned method; (b) – phased averaged results;[11] (c) – Sree's method.[11]
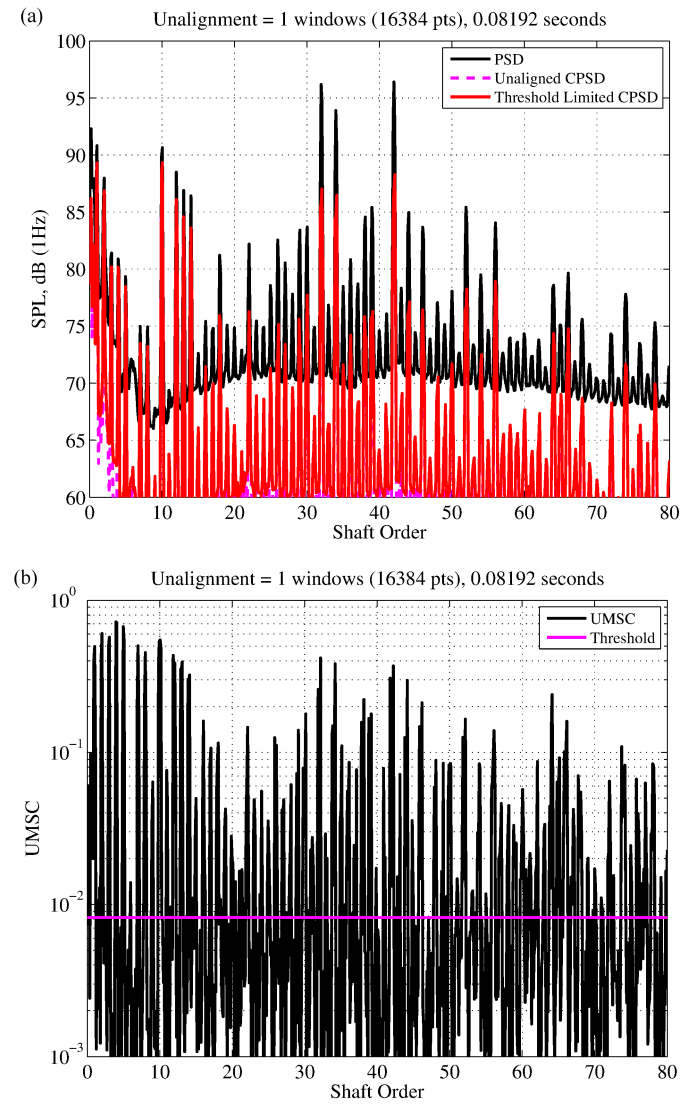
(a)

Unalignment = 1 windows (16384 pts), 0.08192 seconds

(b)

Unalignment = 1 windows (16384 pts), 0.08192 seconds

Figure 3. CROR (reading 470) results: (a) – aligned (black) and unaligned (red, threshold-limited, and magenta) 1 Hz normalized SPL; (b) – *UMSC* **(black) and threshold value (magenta).**
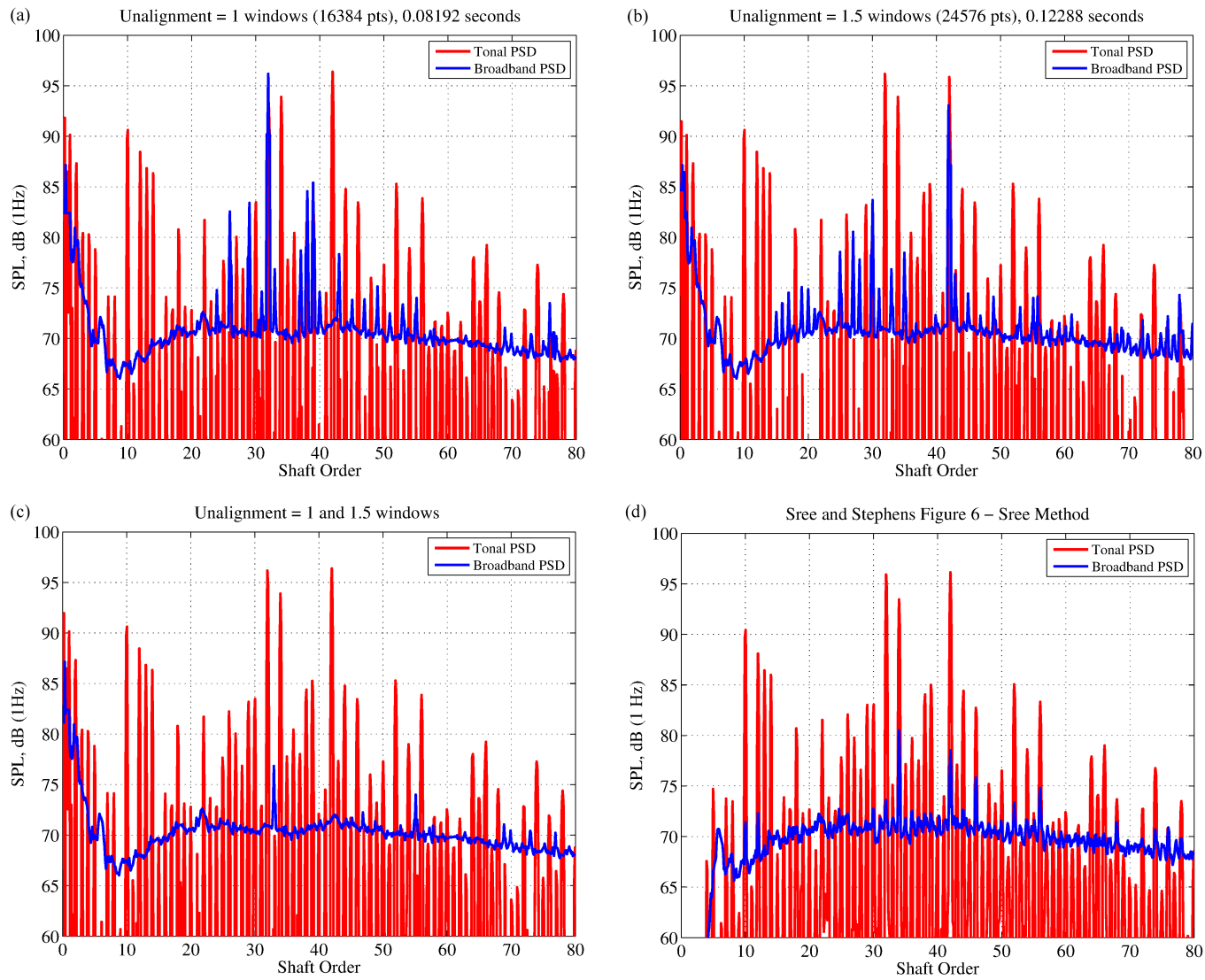
Figure 4. CROR (reading 470) tonal (red) and broadband (blue) SPL spectra: current aligned/unaligned method using (a) – 1 window offset; (b) – 1.5 window offset; (c) – both 1 and 1.5 window offsets; and (d) – Sree's method.[11]
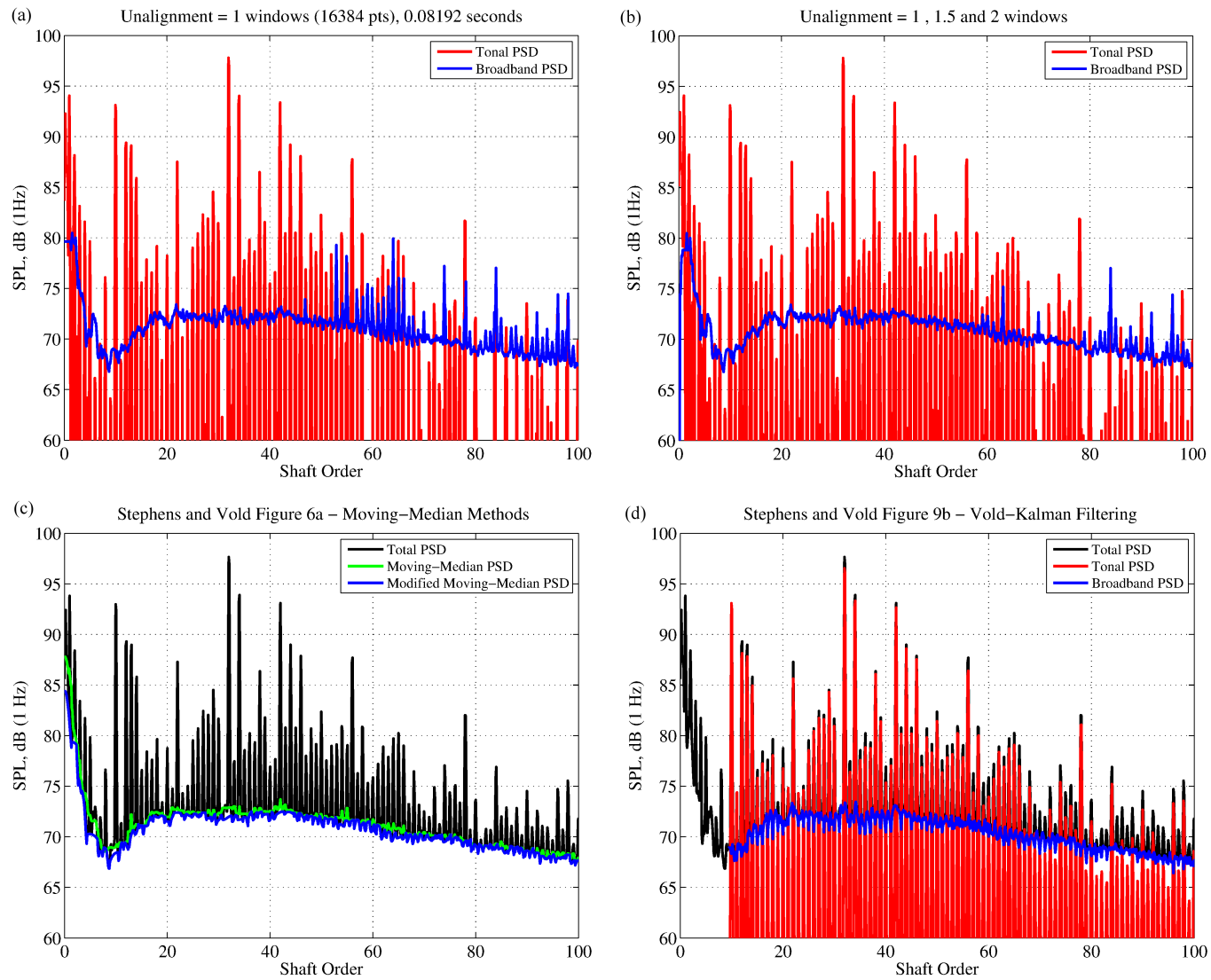
Figure 5. CROR (reading 472) tonal (red), broadband (blue and green), and total (black) SPL spectra: current aligned/unaligned method using (a) – 1 window offset; (b) – 1, 1.5 and 2 window offsets; (c) – moving-median results;[12] and (d) – Vold-Kalman filtering.[12]